Electron spin resonance and exchange paths in the orthorhombic dimer system Sr$_2$VO$_4$

J. Deisenhofer,[1] S. Schaile,[1] J. Teyssier,[2] Zhe Wang,[1] M. Hemmida,[1] H.-A. Krug von Nidda,[1] R. M. Eremina,[3] M. V. Eremin,[4] R. Viennois,[2] E. Giannini,[2] D. van der Marel,[2] and A. Loidl[1]

[1]*Experimentalphysik V, Center for Electronic Correlations and Magnetism, Institute for Physics, Augsburg University, D-86135 Augsburg, Germany*
[2]*Département de Physique de la Matière Condensée, Université de Genève, CH-1211 Genève 4, Switzerland*
[3]*E. K. Zavoisky Physical Technical Institute, 420029 Kazan, Russia*
[4]*Institute for Physics, Kazan (Volga region) Federal University, 430008 Kazan, Russia*

We report on susceptibility and electron spin resonance (ESR) measurements at X- and Q-band frequencies of Sr$_2$VO$_4$ with orthorhombic symmetry. In this dimer system, the V^{4+} ions are in tetrahedral environment and are coupled by an antiferromagnetic intradimer exchange constant $J/k_B \approx 100$ K to form a singlet ground state without any phase transitions between room temperature and 2 K. Based on an extended Hückel tight-binding analysis, we identify the strongest exchange interaction to occur between two inequivalent vanadium sites via two intermediate oxygen ions. The ESR absorption spectra can be well fitted by a single Lorentzian line and the temperature dependence of the ESR intensity, and the dc susceptibility can be modeled by using the Bleaney-Bowers approach for independent dimers. The temperature dependence of the ESR linewidth at X-band frequency can be modeled by a superposition of a linear increase with temperature with a slope $\alpha = 1.35$ Oe/K and a thermally activated behavior with an activation energy $\Delta/k_B = 1418$ K, both of which point to spin-phonon coupling as the dominant relaxation mechanism in this compound.

I. INTRODUCTION

Spin-dimer systems that form a nonmagnetic singlet ground state at low-temperatures are a fascinating class of materials, which, for example, may undergo a spin-Peierls transition[1–4] or may be driven to a magnetic-field induced condensation of magnons.[5] Transition metal oxides provide many of the physical realizations of such systems, such as TlCuCl$_3$,[6,7] BaCuSi$_2$O$_6$,[8,9] and the systems A_3B_2O$_8$ (A = Ba,Sr; B = Cr,Mn).[10–14]

Here, we investigate the vanadium oxide Sr$_2$VO$_4$, which forms two polymorphic structures: a tetragonal one with an alternating spin-orbital order ground state[15–20] and an orthorhombic one with a gapped spin-dimer ground state,[21] which will be in the focus of this study. In orthorhombic Sr$_2$VO$_4$, the V^{4+} ions are in a $3d^1$ configuration and the electron occupies the low-lying e states in tetrahedral environment as sketched in Fig. 1. The material exhibits orthorhombic symmetry with space group $Pna2_1$ and lattice parameters $a = 14.092(4)$ Å, $b = 5.806(2)$ Å, and $c = 10.106(3)$ Å (see Fig. 1).[21] The orthorhombic distortion can be interpreted in terms of a Jahn-Teller distortion, which removes the orbital degeneracy of the V^{4+} ions. No phase transitions have been observed in the temperature range from 4 to 300 K for orthorhombic Sr$_2$VO$_4$. Its susceptibility has been described in terms of a spin-dimer system with a singlet ground state and an antiferromangetic intradimer coupling of about 100 K.[21] However, a clear identification of the superexchange paths corresponding to the magnetic intradimer coupling is not available at present, because the superexchange paths between the structural VO$_4$ units will involve two or more ligands. Such more complicated super-super-exchange (SSE) paths have been found to yield exchange couplings of considerable magnitude and to determine the ground-state properties in a large number of compounds.[22–25]

Here, we investigate orthorhombic Sr$_2$VO$_4$ by magnetization and electron spin resonance experiments. The exchange paths are analyzed by an extended Hückel tight-binding (EHTB) approach and one dominant exchange path via two intermediate oxygen ions is identified. The ESR intensity confirms the dimer approach of the susceptibility, the spin-orbit coupling is estimated from the effective g factor, and the linewidth seems to be governed by a phonon-mediated relaxation mechanism and a thermally activated process.

II. EXPERIMENTAL DETAILS

Ceramic samples were prepared from a Sr$_4$V$_2$O$_9$ precursor[17] by four consecutive reduction and grinding processes at 1100 °C in sealed quartz tubes with metallic Zr as an oxygen getter. The samples were characterized by x-ray powder diffraction using Cu K_α radiation (see Fig. 2) and showed good agreement with the reported orthorhombic symmetry (space group $Pna2_1$) and lattice parameters.[21] We want to mention that the orthorhombic phase of Sr$_2$VO$_4$ can be synthesized with higher purity and is more stable than the tetragonal form.[17,19] Susceptibility measurements were performed using a SQUID magnetometer (Quantum Design). ESR measurements were performed in a Bruker ELEXSYS E500 CW-spectrometer at X-band ($\nu \approx 9$ GHz) and Q-band ($\nu \approx 34$ GHz) frequencies equipped with continuous He-gas-flow cryostats in the temperature region $4 < T < 300$ K. ESR detects the power P absorbed by the sample from the transverse magnetic microwave field as a function of the static magnetic field H. The signal-to-noise ratio of the spectra is improved by recording the derivative dP/dH using lock-in technique with field modulation.
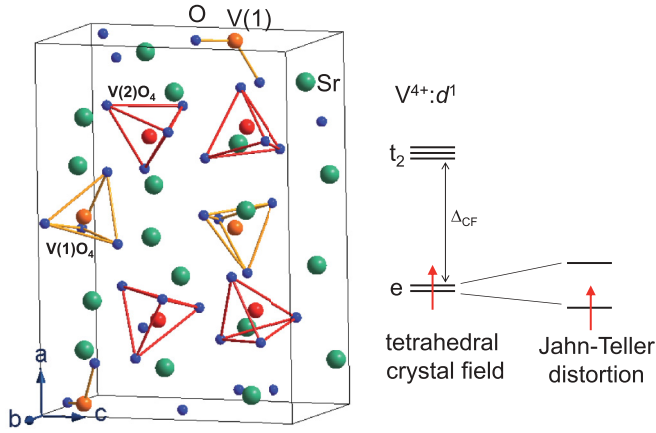
FIG. 1. (Color online) (Left) Unit cell of orthorhombic Sr_2VO_4 with space group $Pna2_1$ (see Ref. 21), showing the tetrahedral coordination of the two inequivalent vanadium sites V(1) (yellow middle-sized spheres) and V(2)(red middlesized spheres). Oxygen and strontium ions are depicted as small blue and large green spheres, respectively. (Right) Schematic of the splitting of the V^{4+} d levels as described in the text.

III. EXPERIMENTAL RESULTS AND DISCUSSION

A. Magnetic susceptibility

Let us now consider the temperature dependence of the molar susceptibility of Sr_2VO_4 as shown in Fig. 3. The susceptibility has been reported previously by Gong and coworkers who described the system in terms of antiferro-magnetically coupled spin dimers with a singlet ground state.[21] We follow this approach to analyze the molar susceptibility χ_m determined from the magnetization M measured in an applied magnetic field $H = 1$ kOe in the entire temperature range and we use

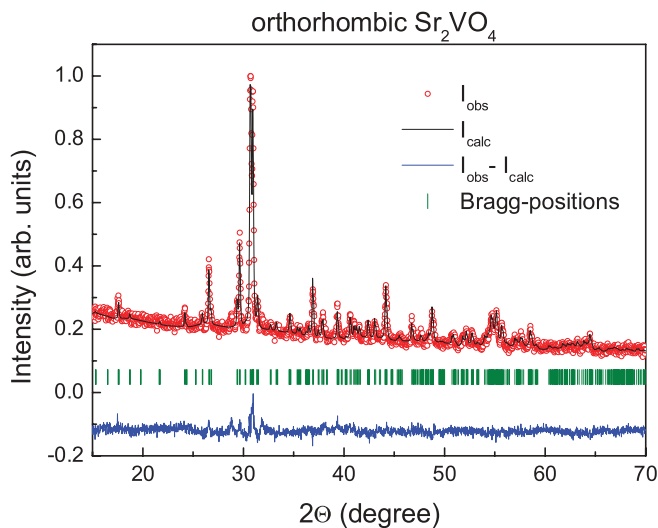$$\chi = \chi_0 + \chi_C + \chi_{BB}, \quad (1)$$

FIG. 2. (Color online) Room-temperature x-ray diffraction pattern of orthorhombic Sr_2VO_4 (open circles) together with the result of the data refinement (black solid line). The difference between experimental and calculated intensities is shown at the bottom, the expected Bragg positions are indicated as green vertical bars.
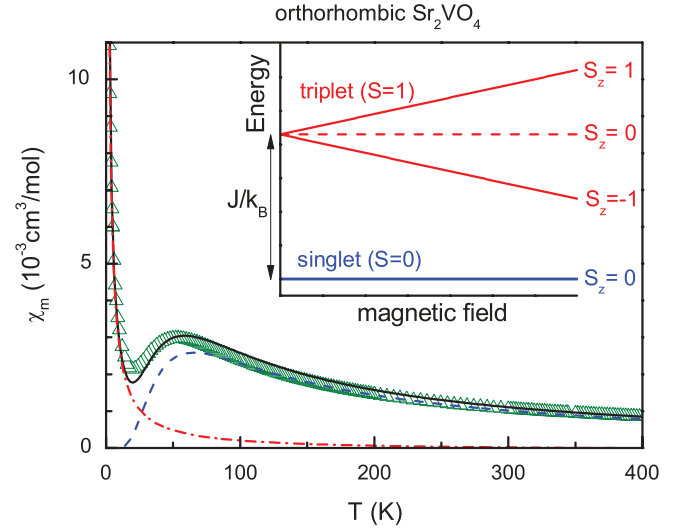

FIG. 3. (Color online) Temperature dependence of the molar susceptibility for orthorhombic Sr_2VO_4 measured in a magnetic field of $H = 1$ kOe. The solid line is a fit using Eq. (1), the dashed and dash-dotted lines correspond to the Curie and dimer contribution of Eq. (1), respectively. The inset shows the corresponding energy level scheme of a spin dimer with antiferromagnetic exchange coupling J as a function of the applied magnetic field.

with a Curie contribution $\chi_C = C/T$ (dash-dotted line in Fig. 3) due to unbound spins and magnetic impurities, a temperature independent contribution χ_0, and the dimer susceptibility χ_{BB} as derived by Bleaney and Bowers (BB) (dashed line in Fig. 3):[26]

$$\chi_{BB}(T) = \frac{Ng^2\mu_B^2}{k_BT}[3 + \exp(J/k_BT)]^{-1}. \quad (2)$$

Here, J denotes the intradimer exchange coupling, g is the effective g factor of the vanadium ions, and μ_B is the Bohr magneton. The BB equation is valid in the case $g\mu_BH \ll k_BT$, i.e., where the Zeeman splitting is small compared to the thermal energy, which is fulfilled in the investigated magnetic field and temperature range. The g factor was fixed to the experimental value $g = 1.89$ observed in the X-band ESR measurements with resonance field of the same order of magnitude as the one applied to measure the susceptbility (see below). The obtained fit parameters are $J = 104K$, $\chi_0 = -1 \times 10^{-4}$ cm^{3}mol^{-1}, which is of the typical order of magnitude for a diamagnetic contribution, and $C = 0.028$ cm^{3}K mol^{-1}, corresponding to about 7% unpaired spins. The maximum of the susceptibility is not perfectly described by this fit with a fixed experimental g value, which might indicate the importance of further exchange couplings between the magnetic dimers. Adding an additional effective interdimer contribution[23] with coupling J' to Eq. (2) leads to an improved fit of the data (not shown), the obtained fit parameters of J and J' are, however, of comparable magnitude which in return discards this approach.[27] Given the fact that the obtained value for the intradimer exchange $J = 104K$ is in agreement with literature[21] and corresponds nicely to a magnetic excitation peaked at 8.6 meV observed by neutron scattering,[28] we think that the model given by Eq. (1) is presently the best parameterization of the experimental
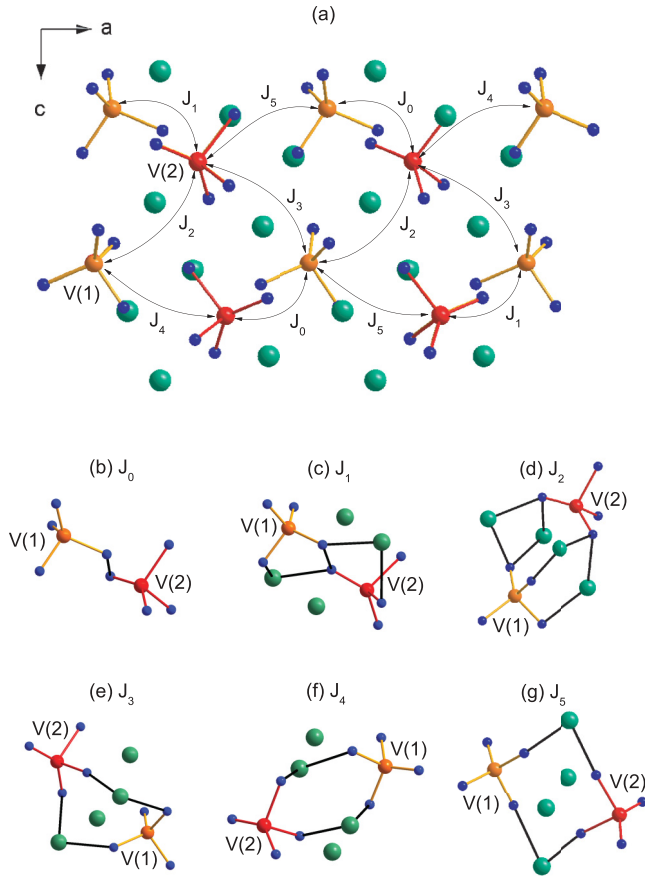
FIG. 4. (Color online) (a) Projection of the orthorhombic lattice structure of Sr_2VO_4 with space group $Pna2_1$ on the ac plane.[21] The exchange paths between neighboring V ions are denoted by the corresponding exchange constants J_0-J_5 in the sequence of increasing V$\cdots$V distance. (b)–(g) Spin dimers associated with these exchange paths. The large, middle, and small spheres show Sr, V, and O atoms, respectively. The two crystallographically inequivalent V ions are denoted as V(1) and V(2), respectively.

susceptibility. From the structural arrangement, however, it is not clear which of the possible exchange paths corresponds to this dominant exchange-coupling constant. Therefore we performed an EHTB analysis of the exchange paths, which will be discussed in the following.

B. Analysis of the exchange paths

Six distinct exchange paths with exchange couplings J_0-J_5 and increasing distance between the vanadium ions can be identified in the structure of Sr_2VO_4 (see Fig. 4 and Table II). The interaction between the magnetic orbitals of two ions in a spin dimer gives rise to two molecular orbitals with an energy splitting Δe. In the spin-dimer analysis based on EHTB calculations,[22,29] the strength of an antiferromagnetic exchange interaction between two spin sites is estimated by $J_{AF} = -(\Delta e)^2/U_{eff}$, where the effective on-site repulsion U_{eff} is taken to be constant. Therefore the trend in $(\Delta e)^2$ is taken as a measure of the J_{AF} values. Double-ζ Slater-type orbitals ϕ_i are adopted to describe the atomic $s, p,$ and d orbitals in the EHTB calculations,[22] which depend on two

TABLE I. Exponents ζ_i and valence shell ionization potentials H_{ii} of Slater-type orbitals ϕ_i used for extended Hückel tight-binding calculations. H_{ii} are the diagonal matrix elements $\langle\phi_i|H_{eff}|\phi_i\rangle$, where H_{eff} is the effective Hamiltonian. For the calculation of the off-diagonal matrix elements $H_{ij} = \langle\phi_i|H_{eff}|\phi_j\rangle$, the weighted formula as described in Ref. 32 was used. C and C' denote the contraction and diffuse coefficients used in the double-ζ Slater-type orbitals.[22,30,31]

atom	ϕ_i	H_{ii} (eV)	ζ_i	C	$\zeta_{i'}$	C'
V	4s	−8.81	1.697	1.0		
V	4p	−5.52	1.260	1.0		
V	3d	−11.0	5.052	0.3738	2.173	0.7456
Sr	5s	−6.62	1.630	1.0		
Sr	5p	−3.92	1.214	1.0		
O	2s	−32.3	2.688	0.7076	1.675	0.3745
O	2p	−14.8	3.694	0.3322	1.825	0.7448

exponents ζ and ζ' and coefficients C and C'.[31] The atomic parameters used for the EHTB calculations of $(\Delta e)^2$ are summarized in Table I. In the EHTB approach, the effective one-electron Hamiltonian H_{eff} is defined semiempirically by its matrix elements.[22] The diagonal matrix elements are denoted by $H_{ii} = \langle\phi_i|H_{eff}|\phi_i\rangle$. The values of the off-diagonal matrix elements $H_{ij} = \langle\phi_i|H_{eff}|\phi_j\rangle$ were taken from Ref. 32. The parameters of V and O atoms are referred to the previous EHTB calculations on other vanadate compounds,[30] while the rest are taken from the atomic orbital calculations.[22,31]

As suggested in Ref. 21, the exchange paths between neighboring vanadium atoms could be V–O–O–V or V–O–Sr–O–V. According to our calculations, the interactions between second- to fifth-nearest neighboring pairs of V ions [see Figs. 4(c)–4(f)] are significantly increased, when the strontium atoms are considered in the exchange paths. In contrast, the effect of the strontium atoms is negligible for the exchange path J_0 [see Fig. 4(b)]. As shown in Figs. 4(b)–4(f), the solid lines indicate the exchange paths between pairs of V ions corresponding to J_0-J_5. For J_1, the exchange path V–O–O–V is still important due to the relatively small distance between the V ions. For J_2-J_5, the exchange paths via Sr ions are more important. Since the distance between sixth nearest neighboring V ions is quite large, the corresponding exchange interaction J_5 is quite small as obtained in Table I, which indicates that neither the exchange path V–O–O–V nor the V–O–Sr–O–V gives a significant contribution to J_5.

The results of our calculations are summarized in Table II. It shows that the dominant spin-dimer exchange is mediated by the path corresponding to J_0 [see Fig. 4(b)], where the

TABLE II. Values of the V$\cdots$V distance in Å and $(\Delta e)^2$ associated with the exchange path J_0-J_5 in Sr_2VO_4.

path	V$\cdots$V	$(\Delta e)^2$ (meV)^2	J_i/J_0
J_0	4.090	1370	1.00
J_1	4.682	46	0.03
J_2	4.734	210	0.15
J_3	4.978	55	0.04
J_4	5.381	69	0.05
J_5	5.511	15	0.01

distance between two V ions is shortest. It is interesting that the second strongest exchange is not between the second-nearest-neighbor V ions, but mediated along the path with J_2. We want to recall that the exchange constants cannot be fully calculated by the EHTB approach, but the estimate of the relative strength of the exchange coupling Js has been found to describe many systems accurately.[22] However, the presently available data on polycrystalline Sr_2VO_4 does not allow to determine subdominant exchange interactions and compare directly to the above estimates.

C. Electron spin resonance

The absorption spectra of Sr_2VO_4 both at X-band ($\nu \approx$ 9 GHz) and Q-band frequencies ($\nu \approx 34$ GHz) can be described by an exchange-narrowed Lorentzian line shape as shown in the insets of Fig. 5. The temperature dependencies of the obtained fit parameters are shown in Fig. 5. The experimentally observed effective g factor at X-band frequency exhibits a constant value of 1.89 in the temperature range $50 < T <$ 200 K, while the evaluation of the Q-band spectra results in a higher value of 1.92. This difference is assigned to the fact that the ESR absorption signal in a powder sample is a statistical average over the presumably anisotropic spectra
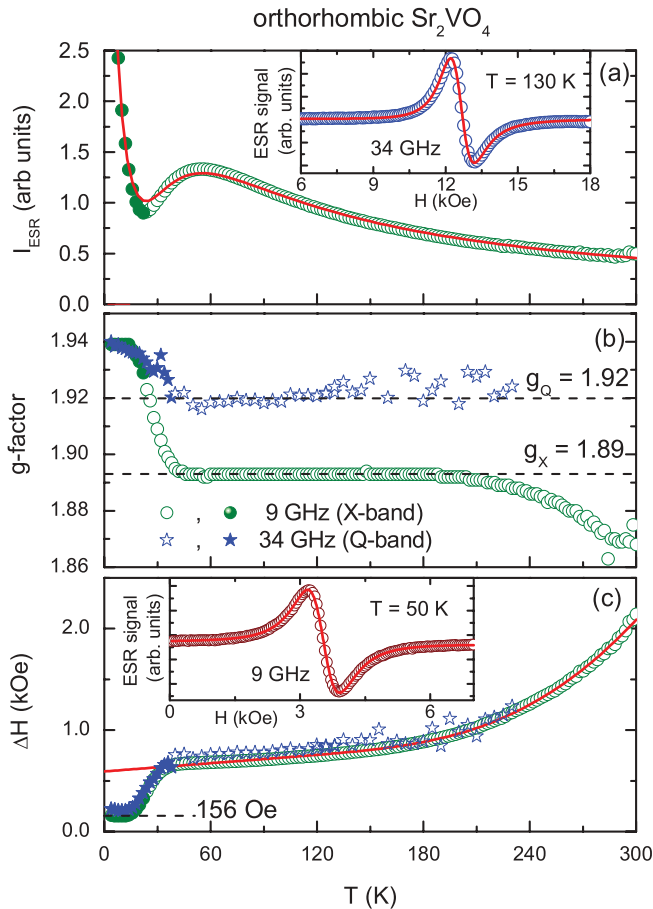

FIG. 5. (Color online) Temperature dependence of (a) the ESR intensity together with a fit using Eq. (1), (b) the effective g factor, and (c) the ESR linewidth in Sr_2VO_4 together with a fit using Eq. (4). The insets show ESR spectra and fit curves with the derivative of a Lorentzian line shape at X-band and Q-band frequencies.

with regard to the orthorhombic crystal axes and the existence of two crystallographically inequivalent vanadium sites (see Fig. 1). At higher resonance frequencies these contributing resonance absorptions will separate more strongly in terms of their respective resonance fields and thus alter the averaged fit parameters obtained by parameterizing the powder spectrum by a single Lorentzian line. The broader distribution of resonance fields also result in an additional broadening of the linewidth via the anisotropic Zeeman interaction[33] and, indeed, an increase of the linewidth of about 80 Oe in the Q-band data with respect of the X-band data is observed for temperatures below about 150 K. Above the linewidth values for both frequencies coincide within the experimental uncertainty. We used the value of 1.89 to fit the susceptibility (see Fig. 3), because the applied external magnetic field is comparable to the X-band resonance field of about 0.3 kOe. Accordingly, the temperature dependence of the X-band ESR intensity I_{ESR} can be well fitted by using Eq. (1) [solid line in Fig. 5(a)] and yields a slightly larger exchange constant $J = 107$ K. These parameters are in agreement with the fit for χ_m and show that the resonance absorption originates from magnetic dipole allowed intratriplet excitations with $\Delta S_z = \pm 1$ (see inset of Fig. 3). The increase of the g factor and the decrease of the ESR linewidth below 30 K signal the depopulation of the excited triplet state and the ESR intensity should drop to zero in the ground state. Instead, the intensity increases towards lower temperatures in a Curie-like fashion (solid circles) indicating that the Lorentzian resonance signals at lowest temperatures with $g = 1.94$ and $\Delta H = 156$ Oe belong to unpaired paramagnetic ions in the sample.

For the intratriplet excitations (open symbols), we find an almost temperature independent g factor $g = 1.89$ between 50 and 150 K. The decrease towards higher temperatures is probably related to the increasing linewidth, which reaches the order of magnitude of the resonance field above 200 K and, hence, imposes a larger uncertainty on the resonance field (or g factor) as a fitting parameter. In first-order perturbation theory, the effective g factor is given by

$$g = 2 - \frac{4\lambda}{\Delta_{CF}}, \quad (3)$$

with the spin-orbit coupling λ and the $e - t_2$ crystal-field splitting parameter Δ_{CF}.[34] Using $g_X = 1.89$, $g_Q = 1.92$, and $\Delta_{CF} = 8900$ cm^{-1} as observed by ellipsometry measurements[35] we estimate $\lambda = 178$–244 cm^{-1} (22–30 meV) in agreement with the values obtained for V^{4+} ions in other compounds.[16,20,34]

The temperature dependence of the ESR linewidth ΔH of the intra-triplet excitations is shown in Fig. 5(c). The linewidth increases monotonously with temperature, between 50 and 170 K only with a moderate slope but for higher temperatures a strong increase sets in, indicating the presence of further relaxation mechanisms. The temperature dependence can be well described by

$$\Delta H = \Delta H_0 + \alpha T + A e^{-\frac{\Delta}{k_B T}}, \quad (4)$$

with $\Delta = 1418(19)$ K, a residual zero-temperature value $\Delta H_0 = 593(5)$ Oe, $\alpha = 1.35(4)$ Oe/K, and $A = 1.23(7) \times 10^5$ Oe at X-band frequency. Fitting the linewidth data at Q-band frequency (not shown) yields the parameters

$\Delta H_0 = 670(25)$ Oe, $\alpha = 1.39(22)$ Oe/K, $A = 3.1 \pm 1.5 \times 10^7$ Oe, and $\Delta = 2.7 \pm 1.1 \times 10^3$ K, which bear a large uncertainty for the exponential parameters as a result of the more limited temperature range and the enhanced scattering of the data at highest obtained temperatures.

Usually, the ESR linewidth in concentrated paramagnetic systems like Sr_2VO_4 is related to spin-flip processes governed by anisotropic spin-spin interactions. For diluted magnetic ions in a nonmagnetic host lattice, a linear increase in the linewidth has been discussed as a result of the modulation of the crystal-electric field by a direct one-phonon process, which modulates the spin-spin relaxation processes via spin-orbit coupling. The slope of this linear increase is expected to strongly depend on the applied magnetic field, e.g., $\propto H^4$ in the case of diluted Kramers ions.[34] This is clearly not the case for Sr_2VO_4, where the linewidth at Q-band frequency of 34 GHz (resonance field of about 12 kOe) is only about 80 Oe (10%) larger than the one at 9 GHz (resonance field of about 3.3 kOe) and exhibits a similar temperature dependence. There are only few experimental and theoretical reports on concentrated magnetic systems with a linear linewidth increase and field-independent slope.[36–41]

Cox and coworkers suggested a mechanism to explain the linear temperature dependence of the linewidth in $Cu(HCOO)_2 \cdot 4 H_2O$, assuming the existence of so-called exchange spin pockets where the spin-up and spin-down sub-levels are mixed by an anisotropic spin-spin coupling exchange parameter D that cancels the magnetic-field dependence of the slope of the linear linewidth increase with temperature.[36] The nature of these exchange pockets is, however, not specified. The same authors suggested the possibility for the linear temperature dependence of the linewidth without magnetic-field dependence due to spin-phonon coupling via modulation of isotropic exchange interactions, but this idea was seemingly discarded by Gill afterwards.[42]

A second mechanism was suggest by Seehra and Castner who argued that the linear temperature dependence in concentrated paramagnets can originate from the phonon modulation of the Dzyaloshinsky-Moriya (DM) interaction, which yields a mixing of the different spin states of exchange coupled pairs.[37,38] In this case, the relevant phonon frequency is about $\propto J/\hbar$ and the one-phonon contribution yields a linear temperature dependence of the linewidth with a slope independent of the value of the magnetic resonance field (or independent of the resonance frequency).

In principle, our results are in agreement with both scenarios, but many details of these two possible mechanisms remain unclear with the former evoking unspecified exchange pockets and the latter assuming a crucial role of the phonon modulated DM interaction for the transition probability between the singlet ground state and excited tripled state. Note that experimentally, we have no indication of the presence of a sizable static DM interaction, but there is no center of inversion between the two inequivalent V sites and a static DM contribution within the dimers could arise.

Moreover, we would like to mention a further possible scenario which is related to a dynamical DM interaction as discussed for $KCuF_3$.[43] A straightforward way to calculate the ESR linewidth in concentrated paramagnets is the method of moments and it is well known that the isotropic exchange interaction (even it is modulated by phonons) commutes with the total spin and, therefore, can not be responsible for the linear temperature dependence of the ESR linewidth. Thus the focus is on the anisotropic exchange interactions. In contrast to the case of a one-phonon process in diluted magnetic systems, the δ function $\delta(\hbar\omega - g\mu_B H)$ does not appear in the thermo-dynamic average of the phonon-modulated second moment. Therefore, not only phonons with frequencies $\hbar\omega_{ESR} = g\mu_B H$ are contributing, but also phonons at higher frequencies, which are closer to the maximum of the phonon density of states. This effect should be related to a local vibrational mode, which modulates the anisotropic exchange contributions or may, for example, induce a dynamical DM contribution as in the case of $KCuF_3$.[43] In the limit $\hbar\omega_{ph} \ll k_B T$ a linear temperature dependence of the linewidth is obtained which is independent of the resonant magnetic field.

A thermally activated contribution has been observed for several low-dimensional magnets[4,43,44] and in the dimer system $Sr_3Cr_2O_8$, where Cr^{5+} ions also have an electronic $3d^1$ configuration in a tetrahedral crystal field.[14] In the latter compound the value of $\Delta = 388$ K is within the phonon frequency range and the contribution was tentatively assigned to stem from a two-phonon Orbach process, where the spin relaxation occurs via an absorption of a phonon to a higher-lying electronic state in the energy range of the phonon continuum. For Sr_2VO_4, the value $\Delta = 1418(19)$ K is too high for phonon modes and rules out the presence of an Orbach mechanism. Since all of the mentioned studies deal with Jahn-Teller active ions, another possible origin of such a thermally activated behavior could be the presence of different Jahn-Teller distortions, which are close in energy, e.g. in case of the one-dimensional magnet $CuSb_2O_6$ (Cu^{2+} with spin 1/2 in octahedral environment) the exponential increase of the linewidth with $\Delta = 1484$ K has been observed on approaching a static-to-dynamic Jahn-Teller transition at 400 K.[44] The value of Δ would then correspond to the energy barrier separating the two Jahn-Teller configurations.

IV. SUMMARY

In summary, we investigated orthorhombic Sr_2VO_4 by electron spin resonance measurements at X- and Q-band fre-quencies and identified the dominating exchange path to occur between two inequivalent vanadium sites via two intermediate oxygen ions using an EHTB analysis. The temperature dependence of the ESR intensity and the magnetization reveal a dimerized singlet ground state with an intradimer coupling constant $J/k_B \approx 100$ K. The effective g factor $g = 1.92$ at 34 GHz (Q band) is slightly larger than the one obtained at 9 GHz (X band), which is assigned to the fact that these values are averages of the g tensors of the two different V sites and the different resonance absorptions are parametrized by a single Lorentzian lineshape. Accordingly, the effective ESR linewidth increases by about 10% when measured at 34 GHz, but at both frequencies the linewidth exhibits an increase with rising temperature, which can be understood in terms of a phonon-modulated spin relaxation yielding a linear increase with slope $\alpha = 1.35$ Oe/K and a thermally activated Arrhenius behavior with an activation energy $\Delta/k_B = 1418$ K, which might be related to the Jahn-Teller distortion of the system.

[1] M. Hase, I. Terasaki, and K. Uchinokura, Phys. Rev. Lett. **70**, 3651 (1993).

[2] R. M. Eremina, M. V. Eremin, V. N. Glazkov, H.-A. Krug von Nidda, and A. Loidl, Phys. Rev. B **68**, 014417 (2003).

[3] A. Seidel, C. A. Marianetti, F. C. Chou, G. Ceder, and P. A. Lee, Phys. Rev. B **67**, 020405(R) (2003).

[4] D. V. Zakharov, J. Deisenhofer, H.-A. Krug von Nidda, P. Lunkenheimer, J. Hemberger, M. Hoinkis, M. Klemm, M. Sing, R. Claessen, M. V. Eremin, S. Horn, and A. Loidl, Phys. Rev. B **73**, 094452 (2006).

[5] T. Giamarchi, C. Rüegg, and O. Tchernyshyov, Nat. Phys. **4**, 198 (2008).

[6] T. Nikuni, M. Oshikawa, A. Oosawa, and H. Tanaka, Phys. Rev. Lett. **84**, 5868 (2000).

[7] C. Ruegg, N. Cavadini, A. Furrer, H. U. Gudel, K. Kramer, H. Mutka, A. K. Habicht, P. Vorderwisch, and A. Wildes, Nature (London) **423**, 62 (2003).

[8] Y. Sasago, K. Uchinokura, A. Zheludev, and G. Shirane, Phys. Rev. B **55**, 8357 (1997).

[9] C. Ruegg, D. F. McMorrow, B. Normand, H. M. Ronnow, S. E. Sebastian, I. R. Fisher, C. D. Batista, S. N. Gvasaliya, C. Niedermayer, and J. Stahn, Phys. Rev. Lett. **98**, 017202 (2007).

[10] E. C. Samulon, Y. Kohama, R. D. McDonald, M. C. Shapiro, K. A. Al-Hassanieh, C. D. Batista, M. Jaime, and I. R. Fisher, Phys. Rev. Lett. **103**, 047202 (2009).

[11] M. Kofu, J.-H. Kim, S. Ji, S.-H. Lee, H. Ueda, Y. Qiu, H.-J. Kang, M. A. Green, and Y. Ueda, Phys. Rev. Lett. **102**, 037206 (2009).

[12] A. A. Aczel, Y. Kohama, M. Jaime, K. Ninios, H. B. Chan, L. Balicas, H. A. Dabkowska, and G. M. Luke, Phys. Rev. B **79**, 100409 (2009).

[13] A. A. Aczel, Y. Kohama, C. Marcenat, F. Weickert, M. Jaime, O. E. Ayala-Valenzuela, R. D. McDonald, S. D. Selesnic, H. A. Dabkowska, and G. M. Luke, Phys. Rev. Lett. **103**, 207203 (2009).

[14] Zhe Wang, M. Schmidt, A. Günther, S. Schaile, N. Pascher, F. Mayr, Y. Goncharov, D. L. Quintero-Castro, A. T. M. N. Islam, B. Lake, H.-A. Krug von Nidda, A. Loidl, and J. Deisenhofer, Phys. Rev. B **83**, 201102 (2011).

[15] H. D. Zhou, B. S. Conner, L. Balicas, and C. R. Wiebe, Phys. Rev. Lett. **99**, 136403 (2007).

[16] G. Jackeli and G. Khaliullin, Phys. Rev. Lett. **103**, 067205 (2009).

[17] R. Viennois, E. Giannini, J. Teyssier, J. Elia, J. Deisenhofer, and D. van der Marel, J. Phys.: Conf. Ser. **200**, 012219 (2010).

[18] H. D. Zhou, Y. J. Jo, J. Fiore Carpino, G. J. Munoz, C. R. Wiebe, J. G. Cheng, F. Rivadulla, and D. T. Adroja, Phys. Rev. B **81**, 212401 (2010).

[19] J. Teyssier, R. Viennois, E. Giannini, R. M. Eremina, A. Günther, J. Deisenhofer, M. V. Eremin, and D. van der Marel, Phys. Rev. B **84**, 205130 (2011).

[20] M. V. Eremin, J. Deisenhofer, R. M. Eremina, J. Teyssier, D. van der Marel, and A. Loidl, Phys. Rev. B **84**, 212407 (2011).

[21] W. Gong, J. E. Greedan, G. Liu, and M. Bjorgvinsson, J. Solid State Chem. **95**, 213 (1991).

[22] M.-H. Whangbo, H.-J. Koo, and D. J. Dai, Solid State Chem. **176**, 417 (2003); M.-H. Whangbo, D. Dai, and H.-J. Koo, Solid State Sci. **7**, 827 (2005).

[23] J. Deisenhofer, R. M. Eremina, A. Pimenov, T. Gavrilova, H. Berger, M. Johnsson, P. Lemmens, H.-A. Krug von Nidda, A. Loidl, K.-S. Lee, and M.-H. Whangbo, Phys. Rev. B **74**, 174421 (2006).

[24] R. M. Eremina, T. P. Gavrilova, A. Günther, Z. Wang, M. Johnsson, H. Berger, H.-A. Krug von Nidda, J. Deisenhofer, and A. Loidl, Eur. Phys. J. B **84**, 391 (2011).

[25] Z. Wang, M. Schmidt, Y. Goncharov, Y. Skourski, J. Wosnitza, H. Berger, H.-A. Krug von Nidda, A. Loidl, and J. Deisenhofer, J. Phys. Soc. Jpn. **80**, 124707 (2011).

[26] B. Bleaney and K. D. Bowers, Proc. R. Soc. A **214**, 451 (1952).

[27] Y. Sasago, M. Hase, K. Uchinokura, M. Tokunaga, and N. Miura, Phys. Rev. B **52**, 3533 (1995).

[28] S. Toth *et al.* (unpublished).

[29] Our calculations were carried out by employing the SAMOA (structure and molecular orbital analyzer) program package (M.-H. Whangbo *et al.*, North California State University, http://www.primec.com/products.htm).

[30] H.-J. Koo, M.-H. Whangbo, P. D. VerNooy, C. C. Toraridi, and W. J. Marshall, Inorg. Chem. **41**, 4664 (2002).

[31] E. Clementi and C. Dai, J. Solid State Chem. **14**, 177 (1974).

[32] J. Ammeter, H.-B. Bürgi, J. Thibeault, and R. Hoffmann, J. Am. Chem. Soc. **100**, 3686 (1978).

[33] B. Pilawa, J. Phys.: Condens. Matter **9**, 3779 (1997).

[34] A. Abragam and B. Bleaney, *Electron Paramagnetic Resonance of Transition Ions* (Clarendon Press, Oxford, 1970).

[35] J. Teyssier *et al.* (unpublished).

[36] S. F. J. Cox, J. C. Gill, and D. O. Wharmbys, J. Phys. C **4**, 371 (1971).

[37] M. S. Seehra and T. C. Castner, Phys. Kondens. Mater. **7**, 185 (1968).

[38] T. G. Castner Jr. and M. S. Seehra, Phys. Rev. B **4**, 38 (1971).

[39] A. Zorko, D. Arcon, H. van Tol, L. C. Brunel, and H. Kageyama, Phys. Rev. B **69**, 174420 (2004).

[40] D. Zakharov, J. Deisenhofer, H. A. Krug von Nidda, A. Loidl, T. Nakajima, and Y. Ueda, Phys. Rev. B **78**, 235105 (2008).

[41] S. Schaile, H.-A. Krug von Nidda, J. Deisenhofer, A. Loidl, T. Nakajima, and Y. Ueda, Phys. Rev. B **85**, 205121 (2012).

[42] J. C. Gill, Rep. Prog. Phys. **38**, 91 (1975).

[43] M. V. Eremin, D. V. Zakharov, H.-A. Krug von Nidda, R. M. Eremina, A. Shuvaev, A. Pimenov, P. Ghigna, J. Deisenhofer, and A. Loidl, Phys. Rev. Lett. **101**, 147601 (2008).

[44] M. Heinrich, H.-A. Krug von Nidda, A. Krimmel, A. Loidl, R. M. Eremina, A. D. Ineev, B. I. Kochelaev, A. V. Prokofiev, and W. Assmus, Phys. Rev. B **67**, 224418 (2003).